frontiers | Frontiers in Earth Science

TYPE Original Research
PUBLISHED 19 January 2023
DOI 10.3389/feart.2022.1017858

OPEN ACCESS

EDITED BY
Chong Xu,
Ministry of Emergency Management, China

REVIEWED BY
Anna Agatova,
V.S. Sobolev Institute of Geology and Mineralogy (RAS), Russia
Yong Li,
Institute of Mountain Hazards and Environment (CAS), China

*CORRESPONDENCE
Ping Wang,
wangping@ies.ac.cn

SPECIALTY SECTION
This article was submitted to Geohazards and Georisks, a section of the journal Frontiers in Earth Science

RECEIVED 12 August 2022
ACCEPTED 31 October 2022
PUBLISHED 19 January 2023

CITATION
Wang H, Wang P, Hu G, Yuan R, Ge Y, Xu B and Shi L (2023), Impact of extreme debris flow-induced paleodamming events on the sedimentological evolution of the middle Yarlung Tsangpo River reaches since the late Pleistocene, Tibet.
Front. Earth Sci. 10:1017858.
doi: 10.3389/feart.2022.1017858

Impact of extreme debris flow-induced paleodamming events on the sedimentological evolution of the middle Yarlung Tsangpo River reaches since the late Pleistocene, Tibet

Huiying Wang, Ping Wang*, Gang Hu, Renmao Yuan, Yukui Ge, Bo Xu and Lingfan Shi

State Key Laboratory of Earthquake Dynamics, Institute of Geology, China Earthquake Administration, Beijing, China

As extreme surface processes, long-term river damming and outburst events can impact sediment supply and transportation in valleys and therefore significantly change the landscape. Lacustrine sediments were identified in the wide Xigaze Valley, in the middle reaches of the Yarlung Tsangpo River in Tibet, an area which has been considered to have been a paleodammed lake. However, the evolutionary process and damming mechanisms associated with this paleolake, and any subsequent impact on sedimentation within the valley, remain unclear. Here, we present a detailed geomorphological and sedimentary analysis of the proposed paleolake area, based on a study of a prominent valley fill found along a section of the Yarlung Tsangpo River and its tributary that flows into it from the south, the Menchu River. This section stretches from Xigaze to Dazhuka. Sedimentary facies analysis of two stratigraphic sections in Renbu Town showed that at least two paleolakes caused by debris flow related to glaciers developed in the Xigaze Valley and that the paleodam was located near the outlet of the Dazhuka Gorge. Chronological constraints suggest that the first damming event occurred between ~48.6 and 33.7 ka in Marine Isotope Stage (MIS) 3 and had a minimum lake surface elevation of ~3,820 m. The second damming occurred between ~24.3 and 12.7 ka during the Last Glacial Maximum (LGM), producing a lake surface elevation of at least ~3,760 m. During the development of the paleolakes in the Xigaze Valley, several small-scale damming and outburst events happened in the upper and middle reaches of the Menchu River, resulting in fluviolacustrine and outburst flood sediments accumulating in the main stream of the Yarlung Tsangpo River and forming thick-fill terraces. We presumed that the paleolakes in the middle reaches of the Yarlung Tsangpo River gradually drained as a result of continuous overflow undercutting instead of outburst flood events, thereby allowing fluvial aggradation of the upper reaches of the paleodam.

KEYWORDS

Yarlung Tsangpo, debris flow, dammed paleolake, sedimentary facies, drainage evolution

Introduction

As the largest drainage basin in the Himalayan orogenic belt on the southern Tibetan Plateau (TP), the Yarlung Tsangpo River has experienced intense tectonic activity, with frequent earthquakes, as well as repeated powerful glacial movements since the Quaternary. Many studies have extensively discussed the relationship between the surface processes of the Yarlung Tsangpo River and tectonic uplift and climatic fluctuations (Burg et al., 1998; Ding et al., 2001; Zeitler et al., 2001, Wang et al., 2002; Korup et al., 2010; Zeitler et al, 2014; Wang et al., 2014). Huge differences in the altitude of the terrain, and strong endogenous and exogenous forces, often cause extreme river blockages and outburst flood disasters precipitated by landslides, moraines/glaciers, and debris flows, which make this area one of the most striking and representative for studying the effects of damming events and evolution of hydrological network (Montgomery et al., 2004; Korup and Montgomery, 2008; Lang et al., 2013; Hu et al., 2018, 2022; Liu et al., 2019; Wang et al., 2021). These can, therefore, be considered a transient response to regional tectonic activity and climate change, as well as an important factor in shaping the fluvial landscape on the tectonically active inland mountainous region.

Lacustrine deposits ranging from thick, silty clay to fine, sandy layers frequently developed in the broad valleys of the middle and lower reaches of the Yarlung Tsangpo River, indicating the existence of dammed paleolakes formed by long-term river blockages (Zhang, 1998). Combined with rift zone activity, intermittent extreme damming events may have jointly shaped the alternating sections of wide valleys and narrow gorges (Yin and Harrison, 2000; Zhang et al., 2016). The most well studied of these phenomena in recent decades has been the Gega Paleolake, which was formed by the repeated damming effect of Zelong Valley glaciers at the entrance of the Tsangpo Gorge, potentially maintaining the stability of the fluvial knickpoint (Montgomery et al., 2004; Zhu et al., 2012; Huang et al., 2014; Liu et al., 2015). The subsequent outburst flooding triggered by dam failure also contributed to the erosion of the landscape of the Tsangpo Gorge (Korup and Montgomery, 2008; Lang et al., 2013). Impounded lakes have also been found in other wide tributary valleys in the middle reaches of the Yarlung Tsangpo River, such as the Jiedexiu Paleolake that developed in the Shannan Valley (Kaiser et al., 2009; Kaiser et al., 2010; Zhu et al., 2013; Han et al., 2017), and the Dazhuka Paleolake, exposed in the Xigaze Valley (Zhu et al., 2013; Hu et al., 2018). However, further work on the evolution and geomorphic implications of damming and outburst events is required.

In the Xigaze Valley, Hu et al. (2004) were the first to identify two dammed paleolakes during the Late Pleistocene and believed that the dam was debris flows located near Xigaze City on the southern banks of the Yarlung Tsangpo River. Thermoluminescence (TL) and radiocarbon (^{14}C) dating of these paleolake sediments gave ages of 25.6–12.3 ka. Zhu et al. (2013) suggested that one dammed paleolake was triggered by a glacial damming event at the entrance of the Dazhuka Gorge between 13 and 12 ka. Hu et al. (2017, 2018) argued that typical lacustrine sediments were also present at Tunda Town in the lower reaches of the Dazhuka Gorge and proposed that a paleolake developed there between 32.3 and 16.2 ka. Major differences remain between different estimations of the spatiotemporal extent, evolutionary processes, and the formation mechanisms of this paleolake. How this extreme surface process shaped the valley's landscape and responded to the tectonoclimatic environment also remains unclear (Korup and Montgomery, 2008; Owen, 2008; Wang et al., 2014). In this study, we conducted a detailed field investigation of the valley's morphology, fluviolacustrine sediments, and moraine and debris flow deposits along the Xigaze to Dazhuka reaches of the Yarlung Tsangpo River. Two stratigraphic sections were selected for detailed sedimentary sequence analysis. We also surveyed fluviolacustrine and outburst flood deposits in the middle and upper reaches of the Menchu tributary river. Combining our findings with chronological optically stimulated luminescence (OSL) results, we reconstructed the evolution and mechanisms behind the paleodamming events and discussed the impact of river blockage on the fluvial landscape of the middle reaches of the Yarlung Tsangpo River.

Study area

The Yarlung Tsangpo River can be divided into upstream, midstream, and downstream sections using the settlements of Lizi and Pai as the dividing points. The middle reaches are nearly 1,400 km long and essentially follow the direction of the Indus–Yarlung Suture (IYS) Zone, passing through a series of nearly N–S rift zones, such as the Cona–Oiga, Yadong–Gulu, and Dinggye–Xainza rift zones, from west to east (Ding et al., 2001; Wang et al., 2002). The whole river course consists of alternating sections of braided, wide U-shaped valleys and deep, narrow V-shaped gorges (Zhang, 1998). Along their longitudinal profiles, the wide valleys are characterized by gentle slopes, connected with gorges characterized by steep gradients downstream, generating large knickpoints between the wide and narrow sections of valleys (Zhang, 1998; Zhang, 1998; Wang et al., 2017).

The wide Xigaze Valley in the study area in the middle reaches of the Yarlung Tsangpo River is ~150 km long and is

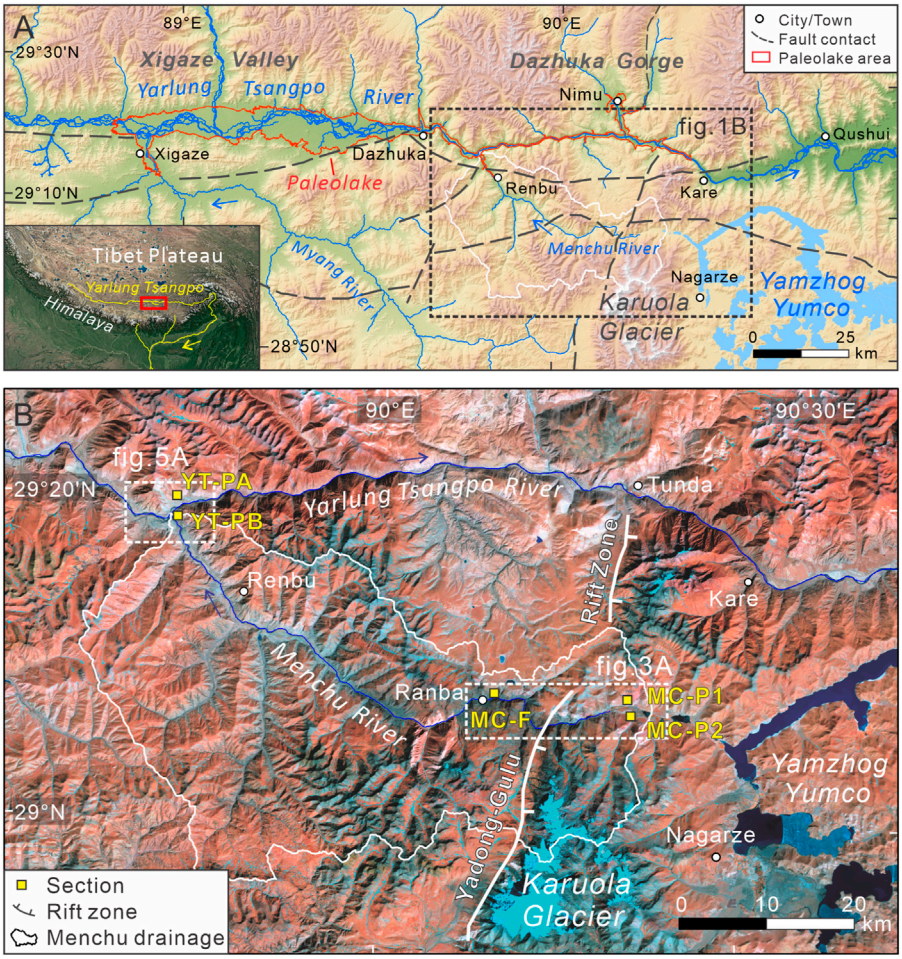

FIGURE 1
Location of the study area, in the middle reaches of the Yarlung Tsangpo River. **(A)**. SRTM 30 m-resolution DEM showing the reaches of the wide Xigaze Valley and Dazhuka Gorge, including paleolake shorelines in red (according to Hu et al., 2018), major faults in gray (modified from Hu et al., 2004), and Menchu River watershed in white. **(B)**. Landsat 8 image (http://ids.ceode.ac.cn/query.html) of Dazhuka Gorge, showing locations of the Yadong–Gulu Rift Zone and study sites (yellow squares) along the Yarlung Tsangpo and Menchu river courses.

dominated by braided and anastomosing channels, with the broadest channel reaching a width of 8–10 km (Figure 1A, Figure 2). The valley is mainly composed of exposed alluvial fans and river terraces, with lacustrine sediments. The river course gradually becomes narrower and deeper from Dazhuka Town onward, before it enters the Dazhuka Gorge area, where the N–S-trending Yadong–Gulu Rift Zone develops (Ha et al., 2019). In the Dazhuka Gorge area, the differential between the altitudes of the mountains on each riverside difference reaches 1,500 m, with exposed bedrock, landslides, and rock avalanche deposits. The river channel becomes wider and gentler in the middle of the rift zone near Nimu Town, where it is characterized by fluvial sands and gravels (Figure 1B). A major tributary on the southern side of the Xigaze Valley, the Menchu River originates from Lake Yamzho Yumco to the west and flows through the southern continental-type Karuola Glacier and the Yadong–Gulu Rift Zone. After turning northwest, the valley becomes wider, with thick-fill terraces, before finally flowing into the Yarlung Tsangpo River near Renbu Town. The lithology of the northern side of the valley is dominated by Jurassic–Neoproterozoic acidic-medium and acidic igneous rocks. On the valley's southern side, Triassic marine dolomite and Jurassic–Cretaceous clastic rocks, limestones, and carbonates have developed. The valley fill is mainly composed of Neoproterozoic–Quaternary sediments; the lower layers are characterized by metamorphic rocks such as ophiolite and Dazhuka conglomerate from the IYS Zone (Hu et al., 2004; Pan et al., 2004).

The high Himalayas block much of the water vapor transported to the region by the Indian Monsoon, resulting in minimal precipitation on north-facing mountain slopes. At higher altitudes, the Yarlung Tsangpo River carries humid air

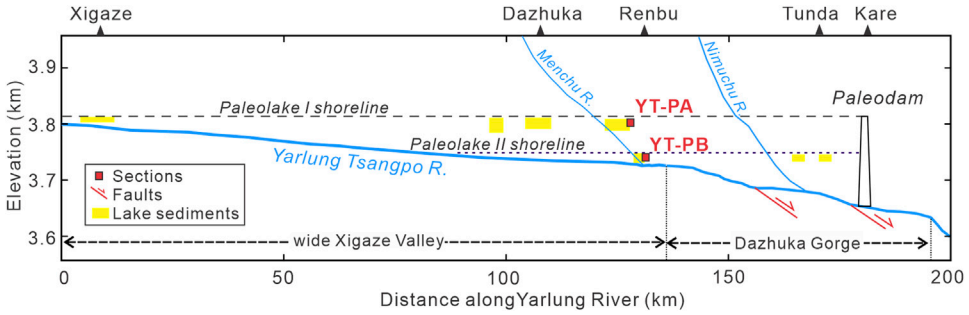

FIGURE 2
Longitudinal profile and location of study sites from Xigaze to the Dazhuka Gorge, in the middle reaches of the Yarlung Tsangpo River.

masses into the TP's interior by acting as a water vapor channel, and precipitation gradually decreases as altitude increases upstream. Overall, there is less rainfall in the middle reaches of the Yarlung Tsangpo River drainage basin (Bookhangen and Burbank, 2010). The glaciers that have developed in the Yarlung Tsangpo River drainage basin can be roughly divided into continental- and marine-type glaciers (Derbyshire, 1982; Zhang et al., 2016). The Karuola Glacier is located to the south of the Menchu River and is a continental-type glacier with an area of ~9.4 km^2, lying at an altitude of 5,042 m above sea level (asl). This glacier is the source of the Myang River, where the Sanwang dammed lake outburst flood event was triggered by an ice avalanche in 1954, with a peak flow of 10^4 m^3/s (Liu et al., 2019). Marine-type glaciers have developed in the southeastern Yarlung Tsangpo River drainage basin, one example of which is the Zelong Glacier, which has itself triggered several river blocking events and formed the Gega dammed lake since the LGM (Montgomery et al., 2004; Huang et al., 2014; Liu et al., 2015). Other river blockage and outburst events have been reported along major tributaries in the Yarlung Tsangpo River drainage basin, such as at the site of the Songzong glacier-dammed paleolake along the Parlung River (Yuan and Zeng, 2012), the landslide-dammed paleolakes along the Lulang and Dongjiu rivers (Wang et al., 2019, Wang et al., 2021), and the Yigong landslide-dammed lake and subsequent outburst flood along the Yigong River course, in 2000 (Turzewski et al., 2019).

Methods

Image analysis and field investigation

Using remote sensing images and digital elevation model (DEM) data interpretation, we analyzed the morphological characteristics of the selected river valley and determined the spatial distribution of river terraces, landslides, and glacial landforms. Combining our findings with those of previous research, we conducted detailed investigations into, and descriptions of, fluviolacustrine sediments and glacial and landslide deposits that have developed in the Xigaze–Dazhuka valley system, and that of the tributary Menchu River. Two river terraces were identified near the entrance of the Dazhuka Gorge (Supplementary Figure S1). Handheld global positioning system (GPS) and topographic mapping were used to obtain the altitudes of the terraces and the paleolakes.

Sedimentological analysis

We investigated the characteristics of the sedimentary deposits in the Xigaze to Dazhuka stretch of the Yarlung Tsangpo River and the Menchu River (Figure 1B, Figure 2). In the Menchu River deposits, we observed the development of possible paleolake and paleodam deposits. The analysis focused on the fluviolacustrine sediments that have developed in the upper reaches of the Menchu River at Jiatang, the glacial and landslide deposits near Zisong, and the outburst flood deposits near Ranba (Figure 3A). Two well-developed fluviolacustrine sedimentary sections were selected for description in the higher and lower terraces near the confluence between the Yarlung Tsangpo and Menchu rivers (Figure 5). Samples were collected to determine the different chronological stages of the dammed paleolakes to help reconstruct the evolution of the damming events.

Sedimentary facies definitions were based on logging and analysis of sedimentary sequence exposures near Renbu (Figure 6, Supplementary Table S1). Changes in grain size, bed thickness, bed contacts, bed geometry, internal sedimentary structures, and soft-sediment deformation structures were logged (Russell et al., 2003; Winsemann et al., 2007; Lang and Winsemann, 2013). Paleoflow direction was determined from analysis of these sedimentary structures, enabling foresets and backsets to be distinguished (Lang and Winsemann, 2013). Sedimentological analysis was undertaken to distinguish lacustrine, lakeshore, subaqueous delta, and alluvial fan sediments, and to differentiate

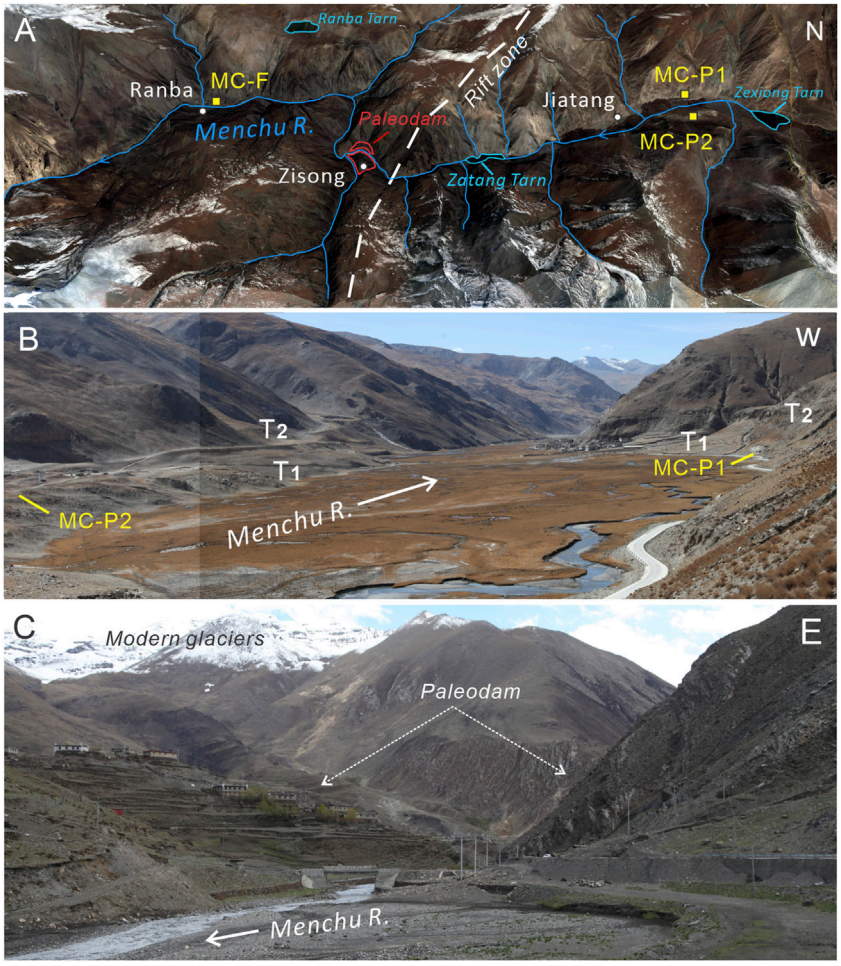

FIGURE 3
Map of study sites in the middle and upper reaches of the Menchu River. **(A)** Image from Google Earth showing the locations of the study sites. **(B)** MC-P1 and MC-P2 sections are located on the lower (T1) and higher (T2) terraces in the upper reaches of the Menchu River, respectively. **(C)** Location of the paleodam that developed near the Zisong Valley, probably triggered by glacier-related debris flows along the valley's southern banks.

between debris flow and turbidity flow processed during subaqueous delta formation (Talling et al., 2012, Table 2). To reconstruct the maximum lake level, we used the altitude of the interface between the subaqueous delta and alluvial fan, rather than the highest altitudinal point of lacustrine or lakeshore sediments (Lang et al., 2017).

Chronological analysis

Six OSL dating samples were collected from Section YT-PA (RB16-51, RB16-53, RB18-2, and RB18-5) and Section YT-PB (RB18-8 and RB18-10) (Table 2). The pretreatment and measurement of OSL samples followed the methodology adopted by Liu et al. (2018). However, almost all the samples exhibited very dim OSL signals due to low luminescence sensitivity and were therefore deemed unsuitable for acquiring precise OSL ages. This phenomenon is common in the Himalayan area, as the quartz grains have only recently been released from source rocks (Spencer and Owen, 2004; Preusser et al., 2009).

Samples were wet-sieved to separate the grain size fractions and treated first with 10% HCl and then with 30% H_2O_2 to remove carbonates and organics, respectively. Next, the residues were etched with H_2SiF_6 for approximately 2 weeks to remove feldspars, followed by further HCl treatment (Lai, 2010). The quartz grains were then mounted at the center of 1-cm diameter stainless steel disks using silicone oil. The concentrations of uranium (U), thorium (Th), and potassium (K) for most samples were measured using neutron activation analysis (NAA) in the Chinese Atomic Energy Institute at Beijing. The water contents were determined by drying a known weight of the

sample and then reweighing and assumed to be 10 ± 2% for sands. OSL samples were analyzed at the Institute of Crustal Dynamics, China Earthquake Administration. Quartz grains of 4e11 mm diameter were measured using a simplified multiple aliquot regenerative-dose (SMAR) protocol.

Sedimentary analysis of damming events in the Menchu River tributary valley

Sedimentation and geomorphology of the river valley

The upper reaches of the Menchu River cross the Karuola Glacier, where the valley is wide and plentiful rich deposits have developed. The middle reaches cross the rift zone over an increasing altitudinal difference, exposing significant quantities of strongly deformed bedrock. The downstream flow turns northwest, through a gradually widening channel and an area of plentiful Quaternary sedimentary deposits, before finally joining the Yarlung Tsangpo River near Renbu Town (Figures 1B, 3A). Two principal river terraces can be identified in the upper Menchu River reaches, and moraine and alluvial fans have developed on both riverbanks (Figure 3B). The main deposits are of fluviolacustrine sediments and alluvial- and glacier-related deposits. Some small overwater lakes such as Zexiong Tarn and Zatang Tarn have also developed, and many larger-scale alluvial fan and debris flow deposits are exposed downstream of these lakes.

The river course in the middle reaches of the Menchu River gradually narrows. The terrain on both riversides increases in altitude, and bedrocks such as mudstone, slate, phyllite, and carbonate begin to be exposed, with strongly deformed lithologies and outcrops inclined at significant angles. We inferred that the Yadong–Gulu Rift Zone runs through this section. The fault is dextral, causing the direction of the river near Zisong Village to migrate northward (Figure 3A). A terminal moraine has developed on the south bank of the Menchu River to the west of Zisong Village, and tongue-shaped deposits are exposed near the riverbank. Combining remote sensing interpretations and field observations, we inferred that the deposits may have accumulated as a result of debris flow from a glacier in the southern branch gully and may have triggered river blockage events (Figure 3C). The paleodam can be found on both sides of the river bank and reaches 150 m above the river surface, which has been modified by terracing and house building (Figure 4A). The paleodam is characterized by thicker, poorly rounded and poorly sorted, dark brown matrix-supported diamicton gravels and sands. The sedimentary materials are relatively loose, with weak or inclined stratifications (Figure 4B). Medium-to fine-grained sands are locally developed in the lower part of the paleodam, with planar and cross laminations, probably formed in a relatively hydrostatic environment during a temporary period of backwater.

Sedimentary sections

We selected and investigated three sedimentary sections for sedimentological analysis in the fluviolacustrine sediments that have developed near Jiatang and Ranba villages in the middle and upper reaches of the Menchu River.

Section MC-P1

Section MC-P1 (90°15′44″E, 29°7′38″N; 4,382 m asl) is located in the T1 terrace upstream of Jiatang Village on the northern perimeter of County Highway 311, at a maximum altitude of 4,390 m asl, and with a thickness of ~7.7 m (Figure 4C). T1 is located ~25 m above the river and is mainly composed of fluviolacustrine sediments. The river at the site of this section exhibits braided channels and includes alluvial deposits from a branch gully on its western side (Figures 3A,B). The bottommost section of the exposure is composed of a ~2 m layer of thick fluvial gravels interspersed with sands, in which horizontal bedding and an imbricate structure have developed. The gravels are principally composed of slate, phyllite, carbonate, and a few granites, with moderate sorting and rounding, roughly similar to the nearby bedrock. The main body of the section is composed of lacustrine sediment that consists of dark gray and light yellow, horizontal laminate clays and silts, with a thickness >5 m at the outcrop, indicating a stable depositional environment (Figure 4D). The variation in dark and light colors may have been caused by different redox environments occurring in different seasons (Hu et al., 2018). The top of the section is covered with light yellow to light gray outwash deposits, and its source would appear to be mainly the moraine that developed on the hillsides. The sediments in the outer part of the outcrop are more solidified, probably resulting from the eluviation of carbonatite.

Section MC-P2

Section MC-P2 (90°16′13″E, 29°7′22″N; 4,419 m asl) is exposed on Terrace T2 on the southern bank of the Menchu River. The altitude of the top surface is ~4,417 m asl (Figure 3B). Many granite boulders are exposed at the terrace's surface. The section in the outcrop is ~2 m thick, mainly exposing gray sands interspersed with light yellow silty clays, representing fluviolacustrine sediments. The fluvial sands are relatively loose, with horizontal and cross bedding, and interspersed with fine-grained clasts. The lacustrine sediments are thin layers of light yellow silty clay, generally approximately 1~2 cm thick (Figure 4E). We discovered fossil shells in the sedimentary section, which are

FIGURE 4
Sedimentary sections in the middle and upper reaches of the Menchu River. **(A)** Remnant paleodam developed in the middle reach, modified by houses and terraces. **(B)** Paleodam deposits developed on the northern bank of the Menqu River. **(C)** Section MC-P1, on Terrace T1. **(D)** Section MC-P1 consists of dark and light silty clays, indicating a stable lacustrine depositional environment. **(E)** Section MC-P2 comprises fine-grained silt and silty sands with thin, clayey layers, indicating a more fluctuating depositional environment. **(F)** Upper part of section MC-F contains outburst flood deposits and is composed of thick, dark gray, coarse-grained sandy layers interspersed with clasts, with parallel bedding developing.

presumed to be the remains of the same species as that found by Hu et al. (2017) in the Xigaze Valley. The top of the section consists of a ~1.5 m thickness of well-rounded fluvial gravels and sands, in unconformable contact with the fluviolacustrine deposits in the section's lower parts. The gravel bedding is largely characterized by a horizontal stratification and imbricate structure, representing the existence of a braided river depositional environment following the end of any lacustrine sedimentary deposition. Overall, the material in the section is loose, with coarse-grained deposits; the lacustrine sedimentary layers are very thin and exhibit as ascending ripple layers, indicating the presence of a more turbulent depositional environment and higher levels of transport energy than Section MC-P1.

Section MC-F

Section MC-F (90°7′34″E, 29°7′53″N; 4,159 m asl) is exposed next to the road on the eastern side of Ranba Village along the northern banks of the Menchu River (Figure 3A). The study site is located downstream of the gorge, where the river channel becomes slightly wider, and the deposits gradually increase on both banks. Branch gullies on the river's northern banks are highly developed. The section consists of ~10 m of thick, dark gray sediments and has been modified by house building (Figure 4F). The lower part of the section consists of dark gray, fine to medium sands, with horizontal and ascending planar stratification, representing a fluvial deposition environment. The upper part of the section is characterized by thicker, dark gray, poorly rounded and poorly sorted, matrix-supported diamicton coarse sands, with parallel and cross-stratification. This layer represents a strong hydrodynamic proximal depositional environment, presumably indicating hyperconcentrated flow deposition by the outburst flooding. The deposition middle part of the flood layer is coarser than the top and bottom part, showing the succession changed from reverse to normally graded, possibly reflecting the process from a rising to waning stage (Marren and Schuh, 2009).

Sedimentary analysis of damming events in the Xigaze–Dazhuka stretch of the Yarlung Tsangpo river valley

Sedimentary sections of dammed lakes

Two principal lake terraces have developed along the Xigaze stretch of the Yarlung Tsangpo River Valley (Supplementary Figure S1). The higher terrace, T2, is widely developed and is ~100 m above the river near Renbu Town; this terrace is principally composed of fluviolacustrine sediments. The bottom of the T2 is composed of thick fluvial gravels and sands. The gravels are well-rounded and sorted, with horizontal and planar crossbedding. The upper part of the terrace is composed of light brown to light yellow clayey layers intercalated with sandy layers, horizontally stratified. A thicker layer of loess and paleosol has developed in T2's upper part. The lower terrace, T1, lies at a height of ~40 m above the river surface. The bottom of the T1 consists of thick fluvial gravels and is in unconformable contact with the upper layer. The upper outcrop is composed of lacustrine sediments, which consist of light yellow silty sands and clay, interspersed with fine gravels. The top layer consists of fluvial gravels and sands and alluvial deposits of varying thickness. Using stratigraphic comparisons, we would speculate that the thick gravel layer exposed at the bottom of T1 may belong to the same stage as the gravel layer in T2, indicating that the river terrace experienced cutting and filling.

Two sedimentary profiles were selected at the confluence of the tributary Menchu River with the Yarlung Tsangpo River, in the transition zone between the wide valley and the narrow gorge (Figures 5A, 6). Lacustrine sediments deposited in a relatively stable environment are typically dominated by clayey to silty sands (Zhu et al., 2013; Liu et al., 2015; Hu et al., 2017, 2018). In this study, the sedimentary sections exhibited varied lithologies and recorded deposition processes that were accompanied by high aggradation rates typical of high energy environments. These deposition episodes were taken to represent periods of paleodamming, as sedimentary deposition can be highly sensitive to repeated damming events and lake surface changes. Cross-laminated and planar bedded sands and silts are frequently exposed in these sedimentary sections, and large quantities of sandy and fine gravel layers have developed in their middle layers, forming sedimentary cycles. A brief overview of the profiles of these sections is presented as follows, using assemblage analysis (LFA1~ LFA4, Table 1).

Section YT-PA

Section YT-PA (89°47′59″E, 29°17′47″N; 3,820 m asl) is located in the section of the upper terrace T2 that runs along the southern bank of the Yarlung Tsangpo River near Renbu Town (Figures 5B, 7A), very close to the section studied by Hu et al. (2018).

Description

LFA1 is mainly dominated by sub-horizontal, thin, medium- to coarse-grained sands, interspersed with fine gravels (Table 1). The LFA1 assemblage in the upper part of the section can be divided into matrix-supported diamicton and gravels (LFA1.1) and fine gravels with coarse sands (LFA1.2). The sediments become progressively coarser and thicker (LFA1.2→LFA1.1) from within the branch gully near the hill, toward the outer main channel. LFA1.1 comprises horizontal and planar bedding of gray to black matrix-supported gravels, with coarse sands (Figure 7B). The gravels are well-rounded and moderately sorted, exhibiting a progressively weaker stratification and planar bedding, and occasionally presenting an imbricate structure. LFA1.2 consists of thick, dark gray sands containing small quantities of matrix-supported, fine-grained diamicton, with well-sorted, parallel bedding and crossbedding, and ascending ripples (Figure 7C). Inclusions containing coarse sand can be seen locally in the sandy layer (Figure 7D).

LFA2 comprises yellow horizontal laminates and ascending ripple layers of silty sand and fine sand, with thin, laminated clayey layers, interbedded with LFA1 (Figures 5B, 7A). LFA2 can also be divided into two sub-facies (Table 1). LFA2.1 comprises medium- to fine-grained sands deformed by perturbation from traction, containing fine-grained diamicton; LFA2.2 consists of less disturbed, fine-grained sands and silts (Figure 7E). These two sub-facies layers have developed in interbedded layers; each layer is ~1–3 m thick, forming four sequential cycles. The LFA2.2 assemblage exposed in the second sequence exhibits a soft, syndepositional deformation from the bottom upward; the LFA2.1 assemblage exposed in the third sequence shows evidence of sand liquefaction.

LFA3 developed at the base of the outcrop and consists of a 1.5-m-thick layer of moderately sorted pebbles and gravels, with crossbedding and an imbricated structure, containing matrix-supported, fine-grained diamicton. LFA3 is in erosional unconformable contact with the upper layer (LFA2.2). LFA 4 is exposed at the top of the outcrop and is composed of a 2–3 m-thick layer of matrix-supported, fine-grained clasts and silty clays (Figure 7B). It contains a ~0.4 m-thick reddish-brown paleosol layer in its lower part, potentially representing the paleoaltitude. Upward of this, calcareous nodules interbedded with fine-grained gravelly sands have developed, with low calcification and weak, horizontal bedding. The topmost part is a 1.5-m-thick layer of gray alluvial deposits.

Interpretation

The pebbles and gravels at the base of LFA3 would appear to record deposition within a fluvial environment. The main body of the section principally comprises an interbedded, dark gray sand to gravel sequence (LFA1) and a yellow silty clay to fine-grained sand sequence (LFA2), possibly indicating the

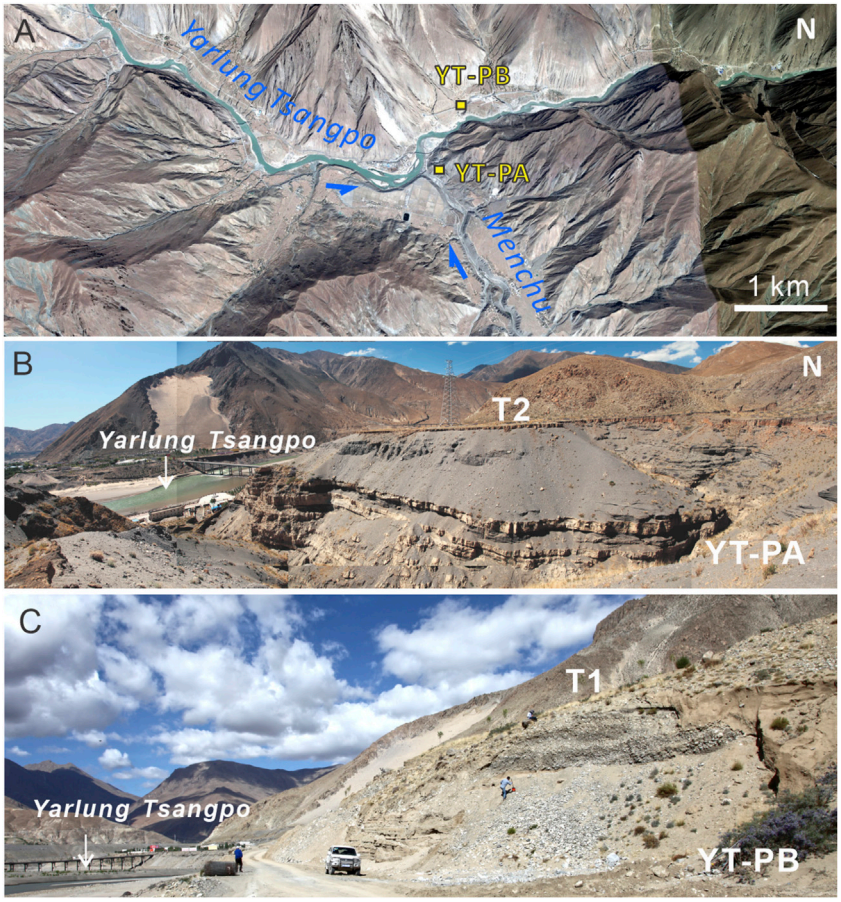

FIGURE 5
(A) Google Earth image of the Renbu Town outcrop, with location of the two stratigraphic sections (yellow squares). **(B)** Field photographs of section YT-PA on Terrace T2, near the confluence of the Yarlung Tsangpo and Menchu Rivers. **(C)** Field photographs of section YT-PB on Terrace T1.

interaction between lacustrine and submerged deltaic or fan deposition with the observed changes between progradation and retrogradation. The section in general can be divided into three sedimentary cycles. The first two lacustrine sedimentary layers at the bottom are composed of silts and clays, indicating a stable depositional environment. Fine-grained clasts are interspersed upward, possibly representing a perturbation of the sedimentary layers by the tributary Menchu River. The hydrodynamic force would have gradually increased as subaqueous fan deposits become the main sedimentary component. The coarse-grained sands, mixed with a few clays and silts, in the third lacustrine sedimentary layer would appear to reflect a relatively unstable depositional environment typical of a later damming stage. The damming event would have caused quantities of deposits from the Menchu River to accumulate at the confluence with the trunk stream of the Yarlung Tsangpo River, forming a thick, gently accumulating platform near Renbu Town. The calcareous paleosol and talus deposits of LFA 4 would have arisen principally from eolian deposition. Hu et al. (2018) suggested that the lacustrine sediments may have become the parent material for the observed paleosols.

Laterally, the sediments closer to the main river channel become more mixed and coarser-grained, with crossbedding, recording a turbulent, high-energy, depositional environment. The sediment becomes finer-grained, with horizontal lamination, further away from the mouth of the channel, suggesting weaker hydrodynamic forces. The two lacustrine sedimentary sub-facies layers (LFA 2.1 and LFA 2.2) would appear to indicate a lake margin environment influenced by weak traction currents. Inclusions filled with matrix-supported, fine-grained diamicton are visible in the sandy layer, probably formed by granular flow or turbidity currents in the pre-delta environment (Johnsen and Brennand, 2006). The lacustrine sediments at the base are in erosional contact with the lower gravelly sediments of LFA 3 formed within a fluvial environment. In contrast to the yellow silty clay and fine-grained sand typical of lacustrine sediments, this section exhibits significant quantities of

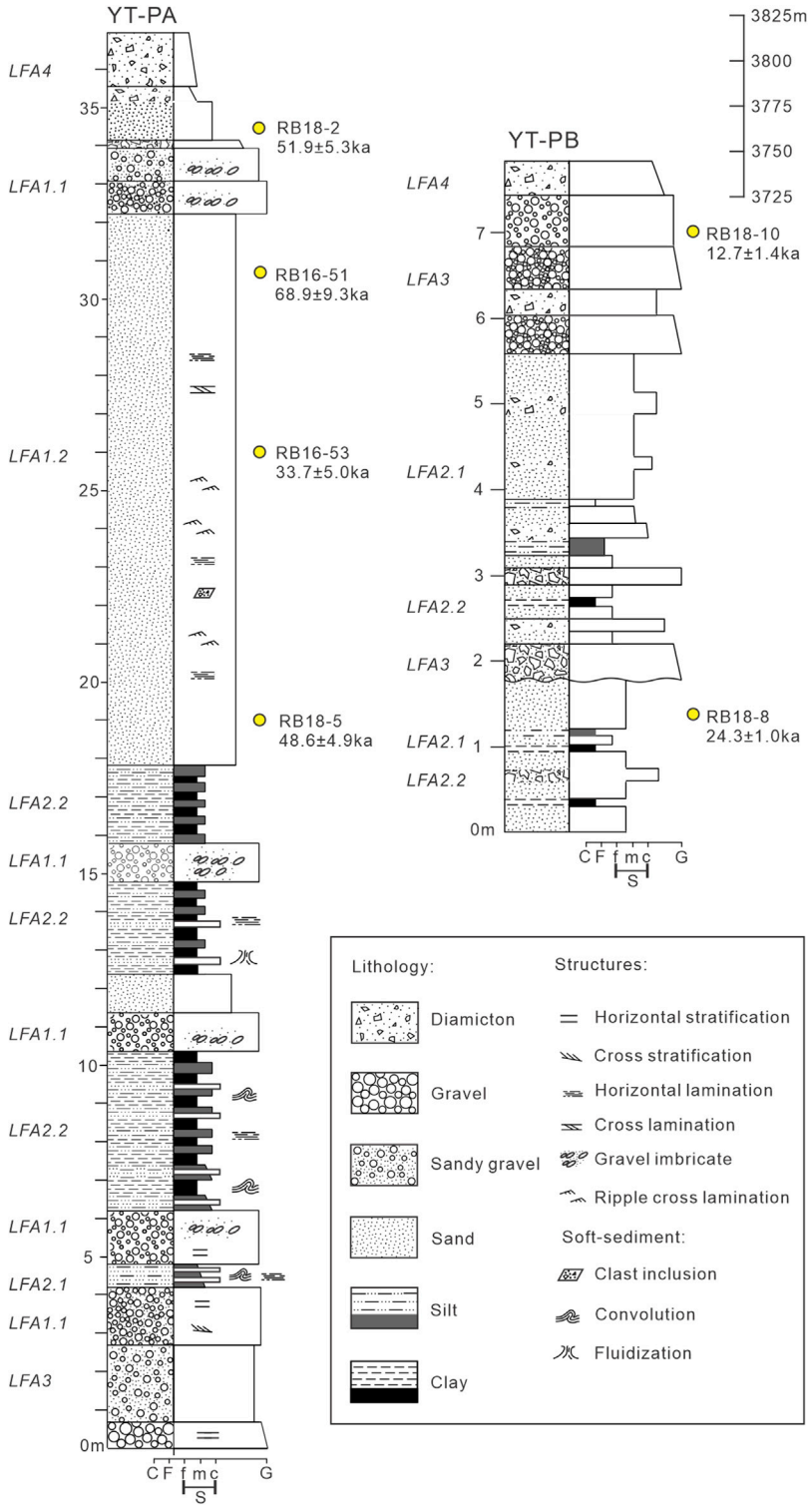

FIGURE 6
Stratigraphic sections YT-PA and YT-PB near Renbu Town in the wide Xigaze Valley (location in Figure 4). Facies association nomenclature is given in Table 1.

TABLE 1 Summary of the lithofacies associations and lithofacies of the Renbu Town sections in the wide Xigaze Valley in the Yarlung Tsangpo River Valley (Shulmeister et al., 2010; Sancho et al., 2018; Wang et al., 2021).

Lithofacies associations		Facies	Lithofacies interpretations
LFA1	LFA1.1	Dark gray, stony silty diamicton and gravels, massive gravels, and clast supported, Dc, Dm, Gm, and Gi	Coarse-grained subdeltaic or subaqueous fan deposition at the confluence, due to progradation by hyperconcentrated flow or debris flows
	LFA1.2	Dark gray, tabular units of horizontal to shallow sand and gravel clinoforms: massive to horizontally or planar bedded fine-grained gravel; massive, horizontal or planar crossbedded sand, Gm, Gi, Gh, Gp, Sm, Sh, Sr1, and Sr2	Finer-grained subdeltaic or subaqueous fan deposition involving cohesionless debris flows and underflow activities
LFA2	LFA2.1	Yellow, silty clays with fine-grained sands interspersed with fine clasts with weak laminations, developing sand liquefaction and soft deposition deformation, Sm, Sh, Sd, Sf, Fm, Fl, and Fh	Slightly deformed lacustrine sediments, shallow lake depositional environment disturbed by river or subaqueous fan
	LFA2.2	Yellow, silty clays and fine-grained sands, developing horizontal, cross, and ripple cross laminations, Sh, Fm, Fl, Fh	Lacustrine deposition dominated by suspension, less disturbed, relatively static water depositional environment
LFA3		Gravels and sands, developing horizontal, tabular, and cross-bedding, imbricate structure, Gi, Gh, Gp, St, Sm, Sh, and Sp	Traction dominated fluvial deposition, disturbed by tributaries
LFA4		Fine-grained clast and sands, silts and clays, Dm, Sm, and Fm	Alluvial and eolian deposition

subaqueous fan and deltaic deposits, with dark gray sands and fine-grained gravels. Combining these findings with our analysis of the outcrop's location and the likely direction of the paleocurrent, we inferred that the tributary Menchu River may have provided quantities of material to the dammed paleolake and surrounding areas.

Section YT-PB

Section YT-PB (29°18′31.78″N, 89°48′15.93″E, 3,796 m asl) is ~2 km northeast of Section YT-PA and lies on the T1 terrace, along the northern bank of the Yarlung Tsangpo River (Figures 5A,C).

Description

LFA2~4 are the assemblages that have principally developed in this section (Figure 6). LFA2.1 comprises medium- to fine-grained sands, with thin layers of fine-grained granules, constituting the main body of lacustrine sediments in the outcrop. Each granular layer is 1–2 cm thick, with poor sorting and rounding, showing occasional disturbance by the tributary river. The thickness of the sandy layer varies from 10 cm to 150 cm, and the lithology varies significantly laterally. The bedding mainly exhibits parallel and cross-laminations, with local, ascending ripples. LFA2.2 comprises mostly 5–10 cm-thick, thin layers of clayey silts, with discontinuous distribution; the sediment is relatively dense, with structureless and planar bedding (Figure 7F).

LFA3 consists of thick granules interspersed with coarse-grained sand in the upper part of the section; these developed on the outer flank of the alluvial fan. The gravel layer as a whole is inclined toward the main channel, with a weakening stratification and an imbricate structure. The grain size is mainly in the range of 3–10 cm, with some larger grains of diameter 30–50 cm, all sub-sorted and moderately rounded (Figure 7G). The LFA4 assemblage can be found in the upper part of the section and consists of 1.5–2 m-thick, matrix-supported, fine-grained clasts and silty clays, with weak stratification.

Interpretation

Overall, the section mainly consists of gravels to silty and clayey sands, typical of lacustrine and subaqueous fan depositional environments. LFA1.2 represents a depositional environment characterized by granular flow or transient turbidity. The low to moderate energy contributions made by landslides within the submerged alluvial fans (Naruse et al., 1997; Johnsen and Brennand, 2004; Wang et al., 2019) potentially reflect a relatively turbulent alluvial or outwash depositional environment. LFA2 comprises the main body of lacustrine sediments. The low clay content, with very thin continuous layers that developed in the lacustrine sediment can be considered typical of a low-energy, shallow lacustrine depositional environment or possibly reflective of disturbance caused by the tributary river, scouring, or turbidity currents (Johnsen and Brennand, 2006). LFA2.1 indicates a depositional progradation caused by relatively strong hydrodynamic conditions, reflecting characteristics typical of subaqueous fans within lake margin environments. LFA2.2 points to weak traction and suspension within a relatively stable depositional environment, typical of a lake bottom. LFA3 is compatible with deposition controlled by traction flow within a braided fluvial environment in the main channel. LFA4 represents post-fluvial deposition and includes alluvial and eolian deposition.

Barrier dams

The exact location of the paleodam is controversial. Hu et al. (2004) suggested that a debris flow occurred in the

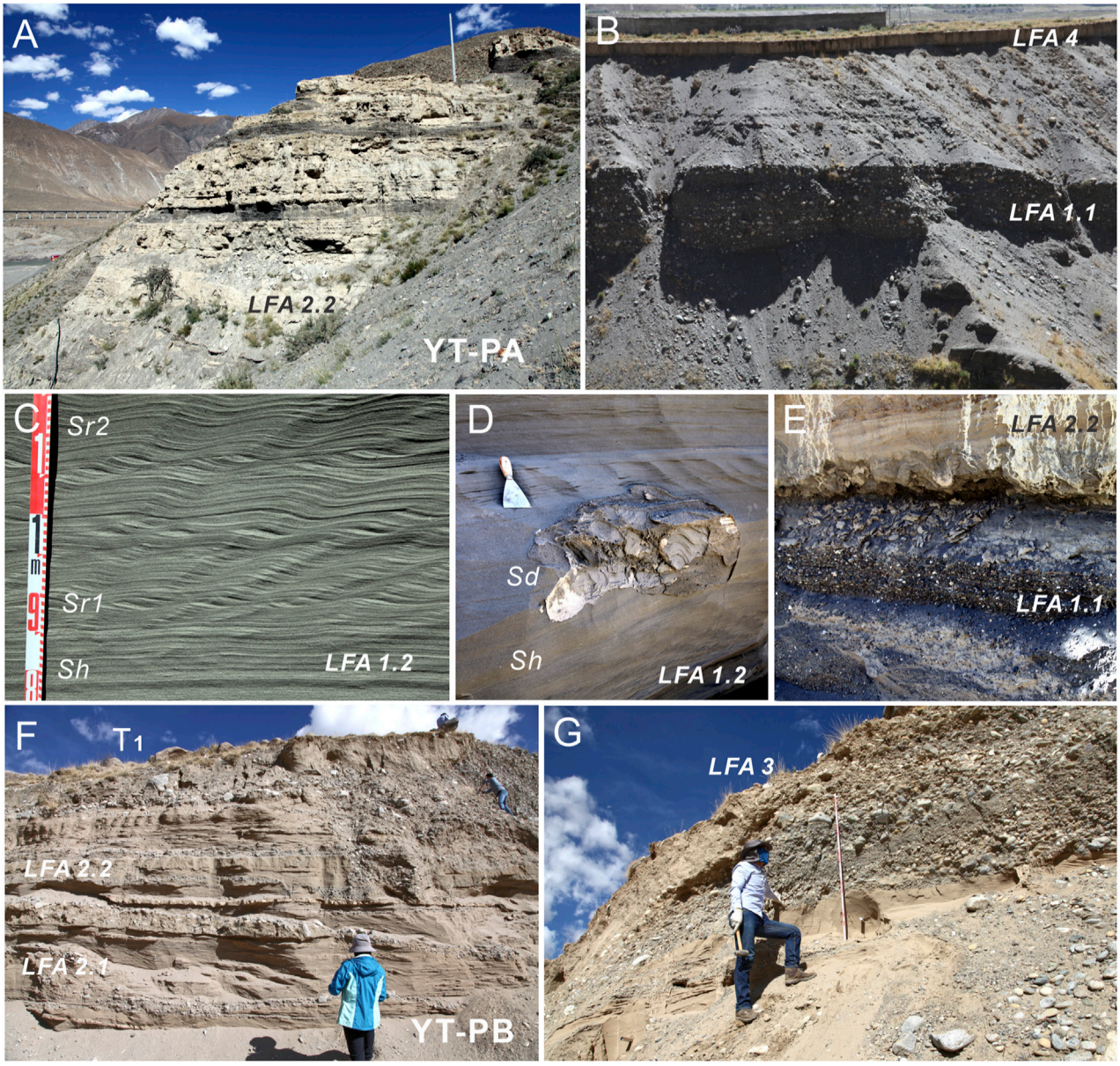

FIGURE 7
Field views of sedimentary facies and lithofacies associations for sections YT-PA and YT-PB. **(A)** Light yellow, lacustrine sediments interbedded with dark gray, subaqueous fan sediments in the upper part of section YT-PA. **(B)** Thick deltaic or fan deposits originating from the Menchu River, dominated by dark gray, medium- to coarse-grained sands and gravels. **(C)** Deltaic or fan deposits composed of medium- to coarse-grained sands, horizontal laminations, interlaminations, and creeping, granular layers. **(D)** Inclusions of diamicton mixed in horizontally laminated, sandy layers. **(E)** Contact between lacustrine strata with a convoluted structure and overlying fluvial, deltaic, gravelly layers. **(F)** Main body of section YT-PB is composed of fine to silty sands, interbedded with silty clays. **(G)** Upper part of section YT-PB consists of fluvial gravels and sandy lens layers.

southern Dazhuka Gorge during the Late Pleistocene and blocked the river, forming two dammed paleolakes. Hu et al. (2017) found thick, gravelly layers near Dazhuka Town and assumed that the observed sedimentary deposition was dominated by a fluvial environment and that the debris flow deposits were too few to have been able to block the channel for a long time.

We conducted field investigations in the Dazhuka Gorge to identify the location of the paleodam. The river course near Dazhuka has a width of ~230 m and lies in the stretch where the river course turns from braided to meandering. Thick, yellow, matrix-supported clasts are exposed on both banks, mainly composed of sub-rounded and sub-sorted gravels; these were assumed to be the debris flow deposits mentioned by Hu et al.

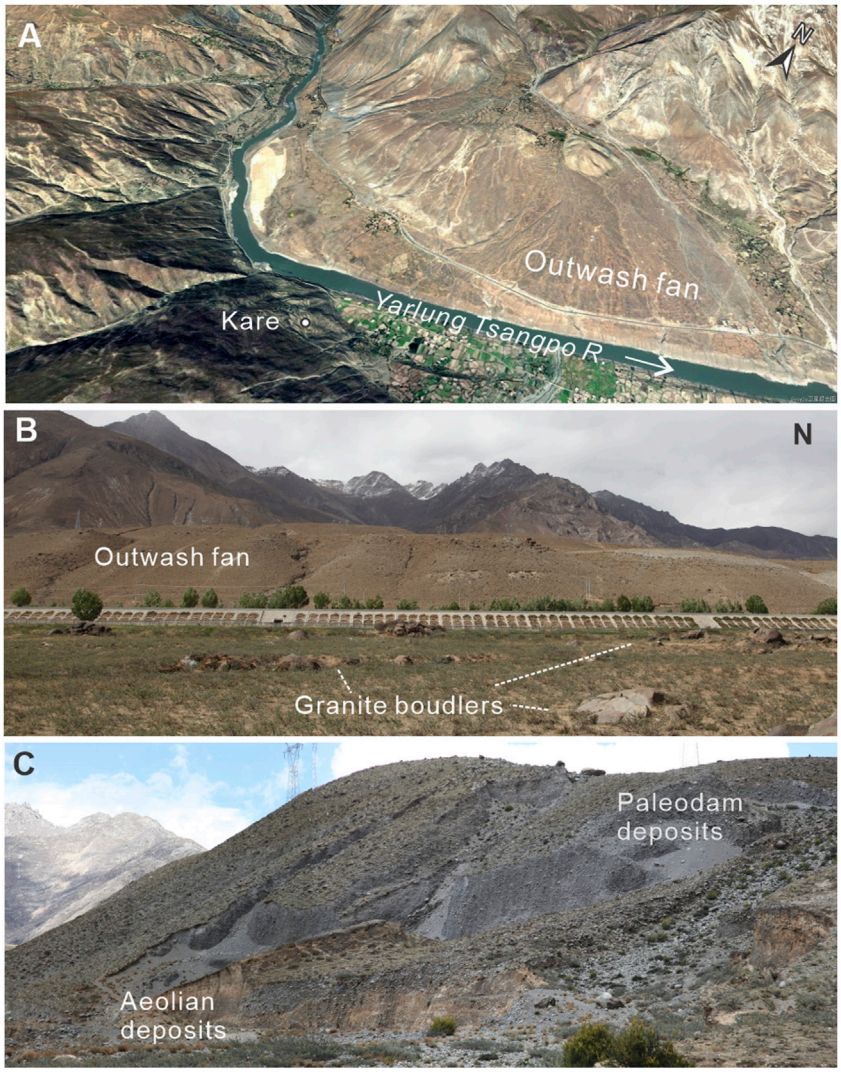

FIGURE 8
Distribution of paleodams near Kare Town downstream of the Dazhuka Gorge. **(A)** Remote sensing image shows outwash fan on the northern banks of the Yarlung Tsangpo River. **(B)** Field photograph of the outwash fan transformed into a thick accumulation platform, with granite boulders exposed nearby. **(C)** Main sedimentary body of the paleodam was composed of dark gray clasts; yellow eolian deposits are exposed in its upper part.

(2004). Our overall observation was that the debris flow deposits were relatively loose and small-scale and that the river channel was wider than that in the gorge area, meaning any long-term blockage would have been less likely. In addition, ~10-m-thick, lacustrine sedimentary layers composed of silty clays and exhibiting a similar sedimentary cycle to sediments in the wider parts of the valley lie exposed in the gorge area, indicating that a unitary paleolake developed in the Xigaze–Dazhuka Valley (Hu et al., 2018). We would, therefore, posit that the possible location of the paleodams was further downstream, in the gorge section.

A large-scale fan consisting of glaciofluvial deposits has developed on the riverbank opposite Kare Town, extending >5 km in length in the direction of the river. This was assumed to be an outwash fan later reformed into a platform (Figure 8A). Granite drift boulders generally >2 m in diameter are scattered at the edge of the outwash platform. Most of the boulders are semi-set on the surface, with some weathering, indicating their early *in situ* time (Figure 8B). The outwash deposits on the platform consist of thick, gray, matrix-supported diamicton, with parallel bedding and crossbedding, and yellow eolian deposits exposed along their margins (Figure 8C). The river channel, from the outwash fan to the exit of the gorge, transforms into a relatively wide, meandering channel and gradually enters the wide Shannan Valley area downstream. We would suggest, therefore, that the paleodam

TABLE 2 OSL dating results for sedimentary samples from the YT-PA and YT-PB sections.

Section	Sample No.	Location	Altitude (m asl)	Depth (m)	U (ppm)	Th (ppm)	K (%)	Water content (%)	Dose rate (Gy/ka)	D_e (Gy)		OSL age (ka)	
										CAM	MAM	CAM	MAM
YT-PA	RB16-51	29.2975°N,89.7990°E	3792	5.0	2.40 ± 0.12	12.70 ± 0.64	1.84 ± 0.09	10 ± 2	3.14 ± 0.09	257.3 ± 24.0	215.9 ± 28.4	82.1 ± 8.0	68.9 ± 9.3
	RB16-53	29.2978°N, 89.7316°E	3810	11.0	3.14 ± 0.16	16.50 ± 0.83	2.05 ± 0.10	10 ± 2	3.65 ± 0.11	162.8 ± 14.2	123.1 ± 17.9	44.6 ± 4.1	33.7 ± 5.0
	RB18-2	29.2966°N, 89.7990°E	3806	3.2	1.46 ± 0.07	11.40 ± 0.57	1.53 ± 0.08	10 ± 2	2.62 ± 0.08	203.8 ± 12.8	135.8 ± 13.3	77.9 ± 5.4	51.9 ± 5.3
	RB18-5	29.2969°N, 89.7988°E	3791	18.0	1.81 ± 0.09	12.20 ± 0.61	2.04 ± 0.10	10 ± 2	3.05 ± 0.09	190.9 ± 9.5	148.0 ± 14.1	62.7 ± 3.7	48.6 ± 4.9
YT-PB	RB18-8	29.3088°N, 89.8044°E	3742	6.5	1.72 ± 0.09	11.30 ± 0.57	2.68 ± 0.13	10 ± 2	3.62 ± 0.12	88.0 ± 2.1	88.0 ± 2.3	24.3 ± 1.0	24.3 ± 1.0
	RB18-10	29.3088°N, 89.8044°E	3739	3.5	1.85 ± 0.09	12.20 ± 0.61	2.75 ± 0.14	10 ± 2	3.84 ± 0.12	68.2 ± 3.9	48.9 ± 5.0	17.8 ± 1.2	12.7 ± 1.4

was the glaciofluvial fan that developed near present-day Kare Town, near the exit of the Dazhuka Gorge, and that the blockage may have been triggered by debris flows from moraines.

Discussion

Chronological analysis

Six OSL samples were collected in this study, and two age models, central age model (CAM) and minimum age model (MAM), were calculated separately (Table 2). The results demonstrate obvious differences between the CAM and MAM for several samples, particularly for the samples from Section YT-PA. This suggests that the quartz grains in these samples may have had insufficient bleaching, which might have caused the CAM dating overestimated. Therefore, we assume that the ages using the MAM method, which focus on the youngest OSL ages, are closer to the sediment burial ages and can reduce the impact of insufficient bleaching (Hu et al., 2015, 2020). Four samples were collected from the sandy layers in Section YT-PA, on T2, and the ages obtained ranged from 68.9 ± 9.3 to 33.7 ± 5.0 ka in MAM results. Samples RB16-51 and RB18-2 were collected from the dark gray sands in the upper part of Section YT-PA, apparently influenced by the Menchu River, which may lead to very unreliable age results. Two samples (RB18-8 and RB18-10) were collected from Section YT-PB. Ages ranged from 24.3 ± 1.0 to 12.7 ± 1.4 ka. All the samples were collected from fluviolacustrine and subaqueous fan deposits, suggesting that their ages can be related to river blockage events.

Using stratigraphic and chronological analysis, we assumed that two paleodamming events likely occurred in the wide Xigaze Valley, latterly forming the two fluvial terraces T1 and T2. The shoreline of the paleolake evident in the higher terrace (T2) lies at an altitude of ~3,820 m asl. According to the dating of samples from the YT-PA Section, the dammed paleolake existed before 48.6 ± 4.9 ka (RB18-5) at the very least and died out after 33.7 ± 5.0 ka (RB16-53). The dating results in this study are unable to provide a better restriction on the ending time of the first damming event because of the disturbance by tributaries on the upper part of the section. The shoreline of the paleolake identified in the lower terrace (T1) lies at an altitude of ~3,760 m asl. Dated samples from Section YT-PB would suggest that the paleolake existed before 24.3 ± 1.0 ka at the very least and died out after 12.7 ± 1.4 ka.

Hu et al. (2004) obtained two ages of 25.6 and 12.3 ka from the lacustrine sediments near Dazhuka, and Zhu et al. (2013) also collected samples in the nearby area, with age results between 12 and 13 ka. Based on their sampling locations and dating results, we assume that the paleolake they identified roughly corresponds to the second paleolake discovered on the T1 terrace in this study. Hu et al. (2018) suggested that the dammed

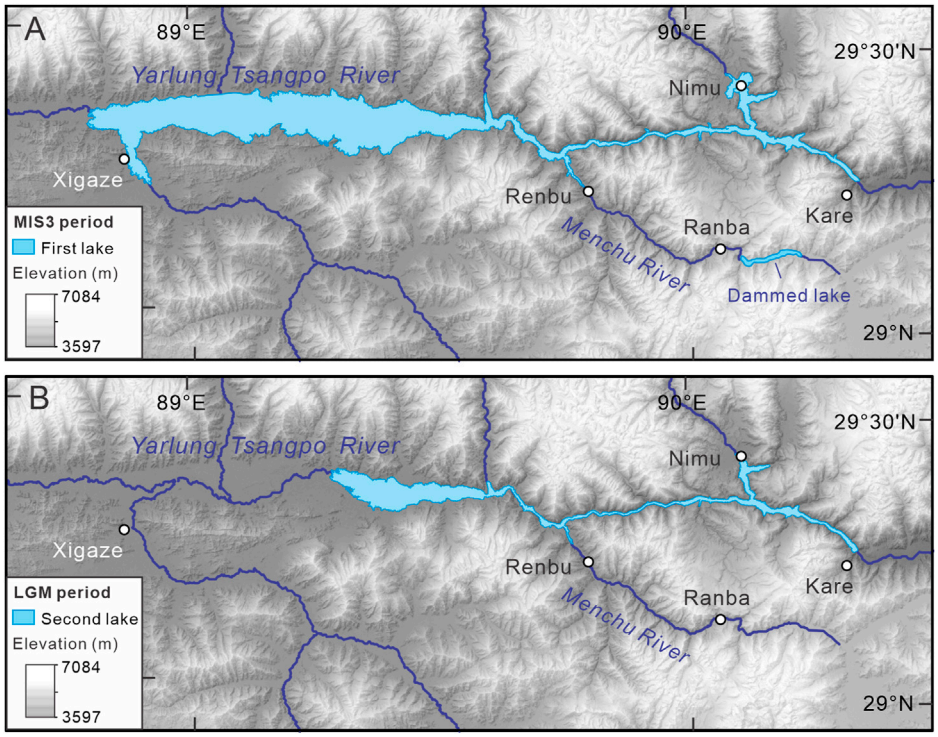

FIGURE 9
Reconstructed extent of the two paleolakes in the Xigaze–Dazhuka section of the middle reaches of the Yarlung Tsangpo River, as determined by 30 m SRTM DEM data to **(A)** the first paleolake during the MIS period and **(B)** the second paleolake during the LGM period.

paleolake in the Xigaze valley formed during >30.2 to 13.2 ka, although the age estimates they derived from three sedimentary sections are inverted and cover a broad age range of ~40 to 1 ka. Comparing the location, elevation, and age data for the sedimentary sections, we assume that the section in Xigaze mentioned by Hu et al. (2018) can correspond to Section YT-PA we described in T2, which is revealed as the first damming event.

Mechanisms of paleodamming events

In a tectonically active mountainous region, long-term river blockage events triggered by landslides, avalanches, debris flows, or glaciers/moraines are often large-scale and likely dominated by local tectonic activity and climate change (Costa and Schuster, 1988; Korup and Tweed, 2007). Combining chronological results of this study with the previous work, we suggest that the time of the two paleodamming events developed within the Xigaze–Dazhuka area roughly corresponds to the Marine Isotope Stage (MIS) 3 and the Last Glacial Maximum (LGM). Glacier advances during the Ice Age may have formed large quantities of glacial-related materials within the gorge. At the same time, continuing tectonic activities in the Yadong–Gulu Rift Zone may have induced landslides or debris flows in the gorge (Wu et al., 2011; Ha et al., 2019). These processes eventually cause glacier-associated materials to move downstream to the river channels and trigger river blockage events. By summarizing the previous studies, we conclude that long-term river blockage events were commonly developed in the Xigaze to Linzhi reach during the Last Glacial Period to the Holocene (Montgomery et al., 2004; Kaiser et al., 2010; Zhu et al., 2013; Hu et al., 2017). This indicates the characteristics of simultaneity for the damming events associated with glacial activity in the middle reaches of the Yarlung Tsangpo River.

The long-term formation of paleodams also requires certain topographical conditions, and usually mountainous areas are relatively easy to sustain long-term river blocking processes (Korup and Tweed, 2007). The middle reaches of the Yarlung Tsangpo River are controlled by the N–S rift zones, causing wide valleys and narrow gorges in the trunk stream, which provide ideal topographical conditions for the development of the dams and dammed lakes (Zhang, 1998). Influenced by the activity of the Yadong–Gulu Rift Zone, the narrow river channel in the Dazhuka Gorge area simply requires a few materials to create tall and stable dams. Meanwhile, the upper wide Xigaze Valley with gentle slope can easily store water from dammed lakes.

Reconstruction of the damming events and evolution of the river terraces

We reconstructed the sedimentary evolution of the dammed paleolakes that developed in the Xigaze–Dazhuka stretch of the Yarlung Tsangpo River Valley (Figure 9). Fluvial sediments had been deposited in the valley before the blockage event. No later than ~48.6 ka, the river channel was blocked and a dammed paleolake was formed, roughly corresponding to MIS3. The river valley at the outlet of the Dazhuka Gorge may have experienced glacial advances at that time. A large-scale outwash fan formed by debris flows related to glacial action developed on the northern riverbank near Kare Town, potentially triggering the damming event. As water levels continued to rise during the damming period, lacustrine sediments began to be deposited, forming the first dammed paleolake. The shoreline of the first paleolake lies at an altitude of ~3,820 m asl, extending to the upper reaches of the Xigaze stretch of the river valley. The lake lasted at least until ~33.7 ka, with the fluvial gravels deposited on the top of the lacustrine sediments, suggesting that the river channel reformed after the demise of the paleolake. The thick lacustrine sediments were scoured and cut by the river, forming new river terraces.

Based on the stratigraphic and lithological characteristics, and sedimentary contact relationships, of the three sections in the Menchu River Valley, we assumed that paleodamming events also occurred in the middle and upper reaches of the tributary Menchu River. After the outburst of the dammed paleolake, significant quantities of fluviolacustrine sediments and outburst flood deposits from the Menchu River Valley would have entered the trunk stream of the Yarlung Tsangpo River, which was in the process of being dammed with a more stable depositional environment. These depositional processes would have led to the development of significant quantities of clastic deposits near present-day Renbu Town, as well as the formation of high, thick accumulation platforms. The interstratification of light yellow, sandy layers and dark gray, sandy and gravelly layers is clear in Section YT-PA. The light yellow sands mainly consist of quartz and feldspar, suggesting they were principally sourced by the trunk stream of the Yarlung Tsangpo River. The material in the dark gray sand and gravel layer mainly contains slate and phyllite, suggesting it was chiefly sourced by the tributary Menchu River. The sedimentary contact relationships show that the dammed paleolake received material continuously from the tributary Menchu River, forming circular sand dikes at the mouth of the tributary. The paleolake appears to have been disturbed by tributaries when it was shallow, forming coarse-grained sand and gravel deposits typical of a subaqueous fan. When the water depth was deeper, lacustrine sediments composed of silty clays from the trunk stream developed (Hu et al., 2018).

The second blockage occurred no later than ~24.3 ka, forming a second dammed paleolake smaller than the first one. Section YT-PB at Renbu Town lies near the end of the paleolake's upper reaches and comprises mostly silty sands, with thin, clayey layers typical of a shallow lake, and interbedded with fluvial sands and gravels. The lacustrine sediment deposits observed in the Nimu Basin lie close to the head of the paleolake, which was located in a rift zone, so the deposits are relatively thick. Hu et al. (2017) investigated a stratigraphic section in the Nimu Basin and found thick, silty clays, typical of a deep lake depositional environment with less fluvial disturbance. The second paleolake would have, therefore, lasted until ~12.7 ka, before gradually draining away. As with the first paleolake, fluvial sediments began to develop on the top of the lacustrine sedimentary layer after the paleolake disappeared.

In the middle and lower reaches of this stretch of the Yarlung Tsangpo River, evidence points to the existence of the Jiedexiu dammed paleolake in the wide Shannan Valley and the Gega dammed paleolake in the wide Milin Valley; their paleodams both appear to have developed toward the entrance to gorges (Montgomery et al., 2004; Han et al., 2017). Conversely, the paleodam that caused the Dazhuka dammed paleolake to develop lay at the outlet of the Dazhuka Gorge. We investigated the gorge areas downstream of the Jiedexiu and Gega paleolakes and found that bedrock was exposed on both banks, with few deposits apparent, and that significant, thick outburst flood deposits were evident downstream of the gorges. In the Dazhuka Gorge, sizeable quantities of material were exposed, including fluvial and alluvial material, with no floodplain accumulation evident downstream of the gorge. We would, therefore, posit that the Dazhuka dammed paleolake may not have experienced a large-scale outburst event. The paleolake more likely drained gradually as a result of continuous overflow and consequent undercutting, explaining the significant quantities of deposits preserved in the gorge area.

Conclusion

Using sedimentary and chronological analyses, we reconstructed two river blockage events during MIS4 and the LGM in the wide Xigaze Valley, in the middle reaches of the Yarlung Tsangpo River on the TP. Both paleodamming events were triggered by glacier-related debris flows, and the resultant paleodams were located near the outlet of the Dazhuka Gorge, near present-day Kare Town. The first river blockage occurred during MIS4 and formed a paleolake between ~48.6 and 33.7 ka, with a minimum lake surface altitude of ~3,820 m asl. The second river blockage occurred during the LGM and formed a smaller paleolake during the ~24.3–12.7 ka period, with a minimum lake surface altitude of ~3,760 m asl. During the damming periods, the tributary Menchu River to the south was also experiencing damming and outburst events, causing significant quantities of deposits to accumulate near the confluence with the Yarlung Tsangpo River near present-day Renbu Town and forming thick accumulation platforms composed of light yellow, fine-grained fluviolacustrine sands and silty clays, interbedded with dark gray, coarse-grained subaqueous fan sands and gravels. The dammed paleolakes may have gradually drained as a result of the

continuous overflow and undercutting of the paleodams, without significant outburst events, preserving sizeable quantities of deposits in the Dazhuka Gorge area.

Data availability statement

The original contributions presented in the study are included in the article/Supplementary Material; further inquiries can be directed to the corresponding author.

Author contributions

Methodology: HYW, RMY, and PW; field investigation: HYW, PW, and BX; OSL sample experiment and dating analysis: HYW, GH, and LFS; writing draft preparation: HYW; writing review and editing: RMY, HG, and YKG; project administration and funding acquisition: HYW and PW.

Funding

This study was financially supported by the State Key Laboratory of Earthquake Dynamics (grant number: LED2021A04), the National Non-Profit Fundamental Research Grant of China (grant number: IGCEA2218) and National field Scientific Observation Research Station Special Project (grant number: NORSLS20-06).

Acknowledgments

The authors acknowledge the editor and reviewers for their contributions and assistances in promoting the manuscript to the current edition.

Conflict of interest

The authors declare that the research was conducted in the absence of any commercial or financial relationships that could be construed as a potential conflict of interest.

Publisher's note

Supplementary material

The Supplementary Material for this article can be found online at: https://www.frontiersin.org/articles/10.3389/feart.2022.1017858/full#supplementary-material

References

Bookhagen, B., and Burbank, D. W. (2010). Toward a complete Himalayan hydrological budget: Spatiotemporal distribution of snowmelt and rainfall and their impact on river discharge. *J. Geophys. Res.* 115, F03019. doi:10.1029/2009jf001426

Burg, J. P., Nievergelt, P., Oberli, F., Seward, D., Davy, P., Maurin, J. C., et al. (1998). The namche barwa syntaxis: Evidence for exhumation related to compressional crustal folding. *J. Asian Earth Sci.* 16 (2-3), 239–252. doi:10.1016/s0743-9547(98)00002-6

Costa, J. E., and Schuster, R. L. (1988). The formation and failure of natural dams. *Geol. Soc. Am. Bull.* 100 (7), 1054–1068. doi:10.1130/0016-7606(1988)100<1054:tfafon>2.3.co;2

Derbyshire, E. (1982). "Glacier regime and glacial sediment facies: A hypothetical framework for the qinghai-xizang plateau," in Proceedings of Symposium on Qinghai-Xizang (Tibet) Plateau, Beijing, China. Geological and Ecological Studies of Qinghai-Xizang Plateau, Beijing (Science Press), 1649–1656.

Ding, L., Zhong, D., Yin, A., Kapp, P., and Harrison, T. M. (2001). Cenozoic structural and metamorphic evolution of the eastern Himalayan syntaxis (Namche Barwa). *Earth Planet. Sci. Lett.* 192 (3), 423–438. doi:10.1016/s0012-821x(01)00463-0

Ha, G., Wu, Z., and Liu, F. (2019). Late quaternary vertical slip rates along the southern Yadong–Gulu Rift, southern Tibetan plateau. *Tectonophysics* 755, 75–90. doi:10.1016/j.tecto.2019.02.014

Han, J. E., Meng, Q. W., Guo, C. B., Shao, Z. G., Wang, J., Yu, J., et al. (2017). Discovery and significance of the lacustrine sedimentation in the middle reach of Yarlung zangbo River in Tibetan plateau. *Geoscience* 31 (5), 890–899. (in Chinese). doi:10.3969/j.issn.1000-8527.2017.05.002

Hu, G., Yi, C. L., Liu, J. H., Wang, P., Zhang, J. F., Li, S. H., et al. (2020). Glacial advances and stability of the moraine dam on mount namcha barwa since the Last glacial maximum, eastern himalayan syntaxis. *Geomorphology* 365, 107246. doi:10.1016/j.geomorph.2020.107246

Hu, G., Yi, C. L., Zhang, J. F., Liu, J. H., and Jiang, T. (2015). Luminescence dating of glacial deposits near the eastern Himalayan syntaxis using different grain-size fractions. *Quat. Sci. Rev.* 124, 124–144. doi:10.1016/j.quascirev.2015.07.018

Hu, H. P., Feng, J. L., and Chen, F. (2017). δ18O and δ13C in fossil shells of Radix sp. from the sediment succession of a dammed palaeo-lake in the Yarlung Tsangpo valley, Tibet, China. *Boreas* 46 (3), 412–427. doi:10.1111/bor.12231

Hu, H. P., Feng, J. L., and Chen, F. (2018). Sedimentary records of a palaeo-lake in the middle Yarlung Tsangpo: Implications for terrace Genesis and outburst flooding. *Quat. Sci. Rev.* 192, 135–148. doi:10.1016/j.quascirev.2018.05.037

Hu, H. P., Liu, J. H., Feng, J. L., Ye, C. S., Gong, Z. J., Lv, F., et al. (2022). Geomorphic processes of a dammed palaeo-lake in the middle Yarlung Tsangpo River, Tibet. *Sci. Total Environ.* 811, 151949. doi:10.1016/j.scitotenv.2021.151949

Hu, J. R., Sun, Z. L., Chen, G. J., Ni, C., Xia, B. B., Liu, H. F., et al. (2004). New results and major progress in regional geological survey of the Xigaze City Sheet. *Geol. Bull. China* 23 (5), 463–470. (in Chinese). doi:10.3969/j.issn.1671-2552.2004.05.010

Huang, S. Y., Chen, Y. G., Burr, G. S., Jaiswal, M. K., Lin, Y. N., Yin, G., et al. (2014). Late Pleistocene sedimentary history of multiple glacially dammed lake episodes along the Yarlung-Tsangpo river, southeast Tibet. *Quat. Res.* 82 (2), 430–440. doi:10.1016/j.yqres.2014.06.001

Johnsen, T. F., and Brennand, T. A. (2004). Late-glacial lakes in the thompson basin, British columbia: Paleogeography and evolution. *Can. J. Earth Sci.* 41 (11), 1367–1383. doi:10.1139/e04-074

Johnsen, T. F., and Brennand, T. A. (2006). The environment in and around ice-dammed lakes in the moderately high relief setting of the southern Canadian Cordillera. *Boreas* 35 (1), 106–125. doi:10.1080/03009480500359145

Kaiser, K., Lai, Z., Schneider, B., Reudenbach, C., Miehe, G., and Brückner, H. (2009). Stratigraphy and palaeoenvironmental implications of Pleistocene and Holocene aeolian sediments in the Lhasa area, southern Tibet (China). *Palaeogeogr. Palaeoclimatol. Palaeoecol.* 271 (3-4), 329–342. doi:10.1016/j.palaeo.2008.11.004

Kaiser, K., Lai, Z., Schneider, B., and Junge, F. W. (2010). Late Pleistocene Genesis of the middle Yarlung Zhangbo Valley, southern Tibet (China), as deduced by sedimentological and luminescence data. *Quat. Geochronol.* 5 (2-3), 200–204. doi:10.1016/j.quageo.2009.01.005

Korup, O., and Tweed, F. (2007). Ice, moraine, and landslide dams in mountainous terrain. *Quat. Sci. Rev.* 26 (25-28), 3406–3422. doi:10.1016/j.quascirev.2007.10.012

Korup, O., and Montgomery, D. R. (2008). Tibetan plateau river incision inhibited by glacial stabilization of the Tsangpo gorge. *Nature* 455 (7214), 786–789. doi:10.1038/nature07322

Korup, O., Densmore, A. L., and Schlunegger, F. (2010). The role of landslides in mountain range evolution. *Geomorphology* 120 (1–2), 77–90.

Lai, Z. (2010). Chronology and the upper dating limit for loess samples from Luochuan section in the Chinese Loess Plateau using quartz OSL SAR protocol. *J. Asian Earth Sci.* 37 (2), 176–185. doi:10.1016/j.jseaes.2009.08.003

Lang, J., Sievers, J., Loewer, M., Igel, J., and Winsemann, J. (2017). 3D architecture of cyclic-step and antidune deposits in glacigenic subaqueous fan and delta settings: Integrating outcrop and ground-penetrating radar data. *Sediment. Geol.* 362, 83–100. doi:10.1016/j.sedgeo.2017.10.011

Lang, J., and Winsemann, J. (2013). Lateral and vertical facies relationships of bedforms deposited by aggrading supercritical flows: From cyclic steps to humpback dunes. *Sediment. Geol.* 296, 36–54. doi:10.1016/j.sedgeo.2013.08.005

Lang, K. A., Huntington, K. W., and Montgomery, D. R. (2013). Erosion of the Tsangpo gorge by megafloods, eastern Himalaya. *Geology* 41 (9), 1003–1006. doi:10.1130/g34693.1

Liu, W., Carling, P. A., Hu, K., Wang, H., Zhou, Z., Zhou, L., et al. (2019). Outburst floods in China: A review. *Earth-Science Rev.* 197, 102895. doi:10.1016/j.earscirev.2019.102895

Liu, W., Hu, K., Carling, P. A., Lai, Z., Cheng, T., and Xu, Y. (2018). The establishment and influence of Baimakou paleo-dam in an upstream reach of the Yangtze River, southeastern margin of the Tibetan Plateau. *Geomorphology* 321, 167–173. doi:10.1016/j.geomorph.2018.08.028

Liu, W., Lai, Z., Hu, K., Ge, Y., Cui, P., Zhang, X., et al. (2015). Age and extent of a giant glacial-dammed lake at Yarlung Tsangpo gorge in the Tibetan Plateau. *Geomorphology* 246, 370–376. doi:10.1016/j.geomorph.2015.06.034

Marren, P. M., and Schuh, M. (2009). Criteria for identifying jokulhlaup deposits in the sedimentary record. *Megaflooding Earth Mars* 225, 225–242. doi:10.1017/cbo9780511635632.012

Montgomery, D. R., Hallet, B., Yuping, L., Finnegan, N., Anders, A., Gillespie, A., et al. (2004). Evidence for Holocene megafloods down the Tsangpo River gorge, southeastern Tibet. *Quat. Res.* 62 (2), 201–207. doi:10.1016/j.yqres.2004.06.008

Naruse, T., Kitagawa, H., and Matsubara, H. (1997). *Lake level changes and development of alluvial fans in Lake Tuz and the Konya basin during the last 24,000 years on the Anatolian plateau, Turkey*. Kyoto: Nichibunken Japan Review, 173–192.

Owen, L. A. (2008). How Tibet might keep its edge. *Nature* 455 (7214), 748–749. doi:10.1038/455748a

Pan, G., Ding, J., Yao, D., Wang, L., Luo, J., Yan, Y., et al. (2004). *Geological map of the qinghai-xizang (Tibet) plateau and adjacent areas*. Chengdu China: Chengdu Cartographic Publishing House. 1500, 000.

Preusser, F., Chithambo, M. L., Götte, T., Martini, M., Ramseyer, K., Sendezera, E. J., et al. (2009). Quartz as a natural luminescence dosimeter. *Earth-Science Rev.* 97 (1-4), 184–214. doi:10.1016/j.earscirev.2009.09.006

Russell, H. A. J., Arnott, R. W. C., and Sharpe, D. R. (2003). Evidence for rapid sedimentation in a tunnel channel, Oak Ridges Moraine, southern Ontario, Canada. *Sediment. Geol.* 160 (1-3), 33–55. doi:10.1016/s0037-0738(02)00335-4

Sancho, C., Arenas, C., Pardo, G., Peña-Monné, J. L., Rhodes, E. J., Bartolomé, M., et al. (2018). Glaciolacustrine deposits formed in an ice-dammed tributary valley in the south-central Pyrenees: New evidence for late Pleistocene climate. *Sediment. Geol.* 366, 47–66.

Shulmeister, J., Thackray, G. D., Rieser, U., Hyatt, O. M., Rother, H., Smart, C. C., et al. (2010). The stratigraphy, timing and climatic implications of glaciolacustrine deposits in the middle Rakaia Valley, South Island, New Zealand. *Quat. Sci. Rev.* 29 (17–18), 2362–2381.

Spencer, J. Q., and Owen, L. A. (2004). Optically stimulated luminescence dating of late quaternary glaciogenic sediments in the upper hunza valley: Validating the timing of glaciation and assessing dating methods. *Quat. Sci. Rev.* 23 (1-2), 175–191. doi:10.1016/s0277-3791(03)00220-8

Talling, P. J., Masson, D. G., Sumner, E. J., and Malgesini, G. (2012). Subaqueous sediment density flows: Depositional processes and deposit types. *Sedimentology* 59 (7), 1937–2003. doi:10.1111/j.1365-3091.2012.01353.x

Turzewski, M. D., Huntington, K. W., and LeVeque, R. J. (2019). The geomorphic impact of outburst floods: Integrating observations and numerical simulations of the 2000 Yigong flood, eastern Himalaya. *J. Geophys. Res. Earth Surf.* 124 (5), 1056–1079. doi:10.1029/2018jf004778

Wang, E. Q., Chen, L. Z., and Chen, Z. L. (2002). Tectonic and climatic element-controlled evolution of the Yarlung Zangbo river in southern Tibet. *Quat. Sci.* 22 (4), 365–373. (in Chinese). doi:10.3321/j.issn:1001-7410.2002.04.009

Wang, H., Cui, P., Liu, D., Liu, W., Bazai, N. A., Wang, J., et al. (2019). Evolution of a landslide-dammed lake on the southeastern Tibetan Plateau and its influence on river longitudinal profiles. *Geomorphology* 343, 15–32. doi:10.1016/j.geomorph.2019.06.023

Wang, H. Y., Wang, P., Hu, G., Ge, Y. K., and Yuan, R. M. (2021). An early Holocene river blockage event on the Western boundary of the namche barwa syntaxis, southeastern Tibetan plateau. *Geomorphology* 395, 107990. doi:10.1016/j.geomorph.2021.107990

Wang, P., Scherler, D., Liu-Zeng, J., Mey, J., Avouac, J. P., Zhang, Y., et al. (2014). Tectonic control of Yarlung Tsangpo gorge revealed by a buried canyon in southern Tibet. *Science* 346 (6212), 978–981. doi:10.1126/science.1259041

Wang, Y., Zhang, H., Zheng, D., von Dassow, W., Zhang, Z., Yu, J., et al. (2017). How a stationary knickpoint is sustained: New insights into the formation of the deep Yarlung Tsangpo Gorge. *Geomorphology* 285, 28–43. doi:10.1016/j.geomorph.2017.02.005

Winsemann, J., Asprion, U., Meyer, T., and Schramm, C. (2007). Facies characteristics of Middle Pleistocene (Saalian) ice-margin subaqueous fan and delta deposits, glacial Lake Leine, NW Germany. *Sediment. Geol.* 193 (1-4), 105–129. doi:10.1016/j.sedgeo.2005.11.027

Wu, Z. H., Ye, P. S., Barosh, P. J., and Wu, Z. H. (2011). The October 6, 2008 Mw 6.3 magnitude Damxung earthquake, Yadong-Gulu rift, Tibet, and implications for present-day crustal deformation within Tibet. *J. Asian Earth Sci.* 40 (4), 943–957. doi:10.1016/j.jseaes.2010.05.003

Yin, A., and Harrison, T. M. (2000). Geologic evolution of the Himalayan-Tibetan orogen. *Annu. Rev. Earth Planet. Sci.* 28 (1), 211–280. doi:10.1146/annurev.earth.28.1.211

Yuan, G. X., and Zeng, Q. L. (2012). glacier-dammed lake in southeastern Tibetan plateau during the Last glacial maximum. *J. Geol. Soc. India* 79 (3), 295–301. doi:10.1007/s12594-012-0041-z

Zeitler, P., Fu, J., Tandon, N., Nadeau, K., Urakami, T., Barrett, T., et al. (2014). Type 2 diabetes in the child and adolescent. *Pediatr. Diabetes* 15 (S20), 26–46. doi:10.1111/pedi.12179

Zeitler, P. K., Meltzer, A. S., Koons, P. O., Craw, D., Hallet, B., Chamberlain, C. P., et al. (2001). Erosion, Himalayan geodynamics, and the geomorphology of metamorphism. *Gsa Today* 11 (1), 4–9. doi:10.1130/1052-5173(2001)011<0004:ehgatg>2.0.co;2

Zhang, D. D. (1998). Geomorphological problems of the middle reaches of the Tsangpo River, Tibet. *Earth Surf. Process. Landf.* 23 (10), 889–903. doi:10.1002/(sici)1096-9837(199810)23:10<889::aid-esp907>3.0.co;2-e

Zhang, J. Y., Yin, A., Liu, W. C., Ding, L., and Xu, X. M. (2016). First geomorphological and sedimentological evidence for the combined tectonic and climate control on Quaternary Yarlung river diversion in the eastern Himalaya. *Lithosphere* 8 (3), 293–316. doi:10.1130/l500.1

Zhu, S., Wu, Z. H., Zhao, X, T., Li, J. P., and Wang, H. (2012). Middle-Late Pleistocene glacial lakes in the grand canyon of the Tsangpo River, Tibet. *Acta Geol. Sin. - Engl. Ed.* 86 (1), 266–283. doi:10.1111/j.1755-6724.2012.00627.x

Zhu, S., Wu, Z. H., Zhao, X. T., and Xiao, K. Y. (2013). Glacial dammed lakes in the Tsangpo River during late Pleistocene, southeastern Tibet. *Quat. Int.* 298, 114–122. doi:10.1016/j.quaint.2012.11.004